

## Coupled Electron-Phonon Modes in Optically Pumped Resonant Intersubband Lasers

H. C. Liu,\* C. Y. Song, Z. R. Wasilewski, and A. J. SpringThorpe

*Institute for Microstructural Sciences, National Research Council, Ottawa, Canada K1A 0R6*

J. C. Cao

*Shanghai Institute of Microsystem and Information Technology, Chinese Academy of Sciences, Shanghai 200050, China*

C. Dharma-wardana, G. C. Aers, D. J. Lockwood, and J. A. Gupta

*Institute for Microstructural Sciences, National Research Council, Ottawa, Canada K1A 0R6*

(Received 4 July 2002; published 20 February 2003)

Intersubband lasing at 12–16  $\mu\text{m}$  based on a  $\text{CO}_2$  laser pumped stimulated resonant Raman process in GaAs/AlGaAs three-level double-quantum-well structures is reported. The presence, or lack of, lasing action provides evidence for resonantly coupled modes of collective electronic intersubband transitions and longitudinal optical phonons. An anticrossing behavior of these modes is clearly seen when the difference between the pump and lasing energies (i.e., Stokes Raman shift) is compared with the subband separation. This work reveals the significance of the strong coupling between intersubband transitions and phonons and raises a new possibility of realizing a phonon “laser.”

DOI: 10.1103/PhysRevLett.90.077402

PACS numbers: 78.67.De, 42.55.Ye, 42.65.Dr, 78.45.+h

New physical phenomena and devices in the infrared and terahertz frequency regions have attracted much interest in recent years. The quantum-cascade laser (QCL) [1] is probably the most prominent and exciting example of new semiconductor devices both in terms of basic physics [2,3] and potential applications [4,5]. Being a unipolar device involving only electrons, the QCL operates by cascading many active stages. In contrast to the QCL, which is electrically pumped, optically pumped intersubband lasing has received only limited attention so far [6–9]. Optical pumping offers the advantage of highly selective excitation of carriers into the desired subband and thus provides a tool for the study of the lasing mechanism, carrier relaxation, and other processes.

In this Letter we report on experimental results from a systematic study of optically pumped infrared lasers based on the resonant intersubband Raman process. The Raman effect is widely used as an optical characterization tool in the study of semiconductors. Most experiments, though, are carried out in the near-infrared to visible spectral region, and very limited experiments were reported so far in the midinfrared [10,11]. The most important feature of the present work is the evidence of resonantly coupled modes comprising collective intersubband transitions (IT) and longitudinal optical (LO) phonons. Coupled modes in semiconductors were reported in the classic paper of Mooradian and McWhorter [12] on Raman scattering in doped bulk GaAs, which provided definitive evidence of coupled electron plasmon-phonon modes. Coupled electronic excitation-phonon modes have also been observed in other solid state systems [13]. Light scattering experiments have been used for the study of GaAs/AlGaAs heterostructures since the early days of the research in this field [14,15].

Our artificial three-level system is realized in a GaAs/AlGaAs asymmetric double quantum well (DQW). The use of the asymmetric DQW provides the flexibility in designing the desired level separations and affords strong dipole-matrix elements among all states. The structure and the Raman lasing characteristics are illustrated in Fig. 1. The Raman laser works by optical pumping from subband  $E_1$  to  $E_3$  and emitting from  $E_3$  to  $E_2$ . In the original (uncoupled intersubband-phonon) picture [9], the separation between  $E_1$  and  $E_2$  is made in near resonance with a given LO-phonon mode having a fixed phonon energy. All transitions are real (as opposed to virtual) and resonant with intersubband separations. If  $\omega_{\text{pump}}$ ,  $\omega_{\text{laser}}$ , and  $\omega_{\text{phonon}}$  are the pump, laser, and LO phonon frequencies, respectively, we then have  $\omega_{\text{pump}} = \omega_{\text{laser}} + \omega_{\text{phonon}}$  for the Raman process. If the pump frequency is varied (within the 1-to-3 absorption linewidth), the lasing frequency must follow by exactly the same amount since the phonon frequency is fixed; i.e.,  $\omega_{\text{pump}} - \omega_{\text{laser}} = \omega_{\text{phonon}} = \text{const}$  for a given LO-phonon mode (see the bottom part of Fig. 1).

To obtain a sufficient gain and output power the DQW is repeated 150 times, separated by wide (20 nm) barriers, center-delta doped with Si to  $3 \times 10^{11} \text{ cm}^{-2}$  with an uncertainty of  $\pm 10\%$ . The aluminum fraction in all AlGaAs barriers is fixed to 35% for all samples. A range of well thicknesses were used: 7.4–8.0 nm for the wide well and 4.7–6.1 nm for the narrow well, with the thin tunnel barrier fixed at 1.13 nm. The modulation doping in the wide barriers results in an electron population of  $3 \times 10^{11} \text{ cm}^{-2}$  in each DQW. The active region is clad by appropriate waveguiding layers [7,8]. The experimental details (see also Ref. [8]) are as follows. The side-pumping cleaved-facet geometry was used. The excitation

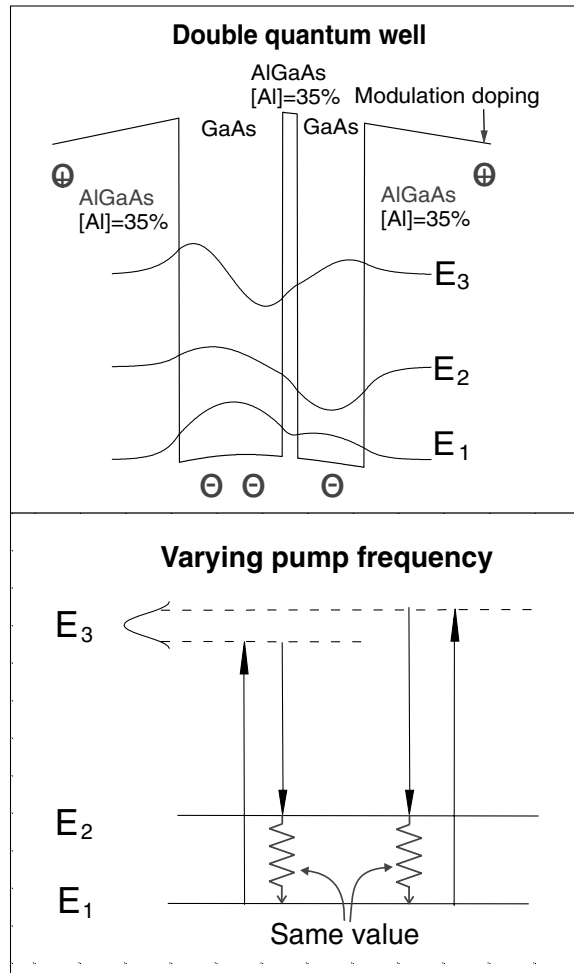


FIG. 1. Top: the calculated double quantum-well potential and wave functions; bottom: an illustration of the Raman lasing characteristics. When the pump frequency is varied within the linewidth of the 1-to-3 transition, the emission frequency changes by the same amount so that the difference is kept the same.

source was a pulsed (50-ns width)  $\text{CO}_2$  laser. The emission spectrum was measured using a Fourier transform interferometer. All lasing experiments were carried out with a sample temperature of 80 K. The lasing characteristics were well established in Refs. [8,9] where clear threshold and spectrometer-limited narrow line behaviors were shown.

For our structure, there are two materials components, GaAs and  $\text{Al}_{0.35}\text{Ga}_{0.65}\text{As}$ . There are therefore three LO-phonon modes: GaAs, GaAs-like, and AlAs-like, with the latter two associated with the  $\text{Al}_{0.35}\text{Ga}_{0.65}\text{As}$  alloy. The characteristics of AlGaAs LO phonons are well studied and documented [16,17]. Taking the empirical expression [17] and the known temperature dependence [16], we obtain 293 (36.3), 280 (34.7), and 383 (47.5)  $\text{cm}^{-1}$  (meV) for the GaAs, GaAs-like, and AlAs-like modes, respectively, at 80 K. We have repeated some of the dielectric continuum model calculations in

Refs. [18,19]. We find that the GaAs, GaAs-like, and AlAs-like “interface” mode frequencies occur very close to their bulk values, practically independent of the changes of the structural parameters in the range used in the present work.

Our first Raman laser worked in near resonance with the AlAs-like phonon with an observed  $\omega_{\text{pump}} - \omega_{\text{laser}} = 386 \text{ cm}^{-1}$  [9], close to the expected AlAs-like phonon value (383) but slightly larger. Since then, we have been investigating a wide range of parameters in the hope to observe Raman lasing with the GaAs phonon. At first sight, the GaAs phonon mediated process may be stronger than the AlAs-like phonon process, because the wave functions overlap the GaAs wells in the DQW. If, however, we adopt the results calculated using the dielectric continuum model [18,19], the interface phonons at both the GaAs and AlAs-like mode energies propagate through the DQW structure with nearly equal strengths and therefore cause 2-to-1 transitions with equal strengths. Our DQW wafers were designed to cover a range of 1-to-2 energy separations and yet to have the 1-to-3 transition falling into the  $\text{CO}_2$  laser tuning range. For the required systematic change, we fix the barriers and vary only the well thicknesses. For the range of well thicknesses used, our samples give a range of 1-to-2 level separation of 28–42 meV which cover the GaAs phonon energy of about 36 meV.

For all samples, emission spectra were collected for different pumping wave numbers (frequencies). The spectra were taken with a spectrometer resolution of  $1 \text{ cm}^{-1}$  and the lasing peak positions were determined with an accuracy better than  $1 \text{ cm}^{-1}$  ( $\sim 0.1 \text{ meV}$ ). Figure 2 shows the emission spectral peak position vs pump position (for about half of the samples to avoid overcrowding), with lasing wavelengths (wave numbers) from 12.0 (830) to 16.4  $\mu\text{m}$  ( $610 \text{ cm}^{-1}$ ). Each type of symbol represents one sample. The gaps with no data in regions of 960, 985 to 1030, and 1060  $\text{cm}^{-1}$  are due to the  $\text{CO}_2$  laser tuning gaps. The inset to the figure shows the transmission spectrum for one sample at room temperature under a multipass  $45^\circ$  geometry. The data in Fig. 2 show that for a given sample the lasing peak shifts very uniformly to higher frequencies as the pump frequency is increased, with a unity slope—a characteristic of the Raman process. This means that for a given sample, the difference between the pump and emission frequencies is constant. Figure 3 plots this constant value of the difference between the emission peak and pumping positions as a function of the 1-to-2 level separation for all samples. Note that the difference plotted here is the Raman shift of the Stokes process. The  $x$  axis of Fig. 3 is based both on the absorption experiment (see the inset to Fig. 2 for one sample) and the calculation, with an error bar of about 1 meV. They are mutually consistent; i.e., the calculated separation corresponds to the difference between the 1-to-3 and 2-to-3 absorption positions, taking into

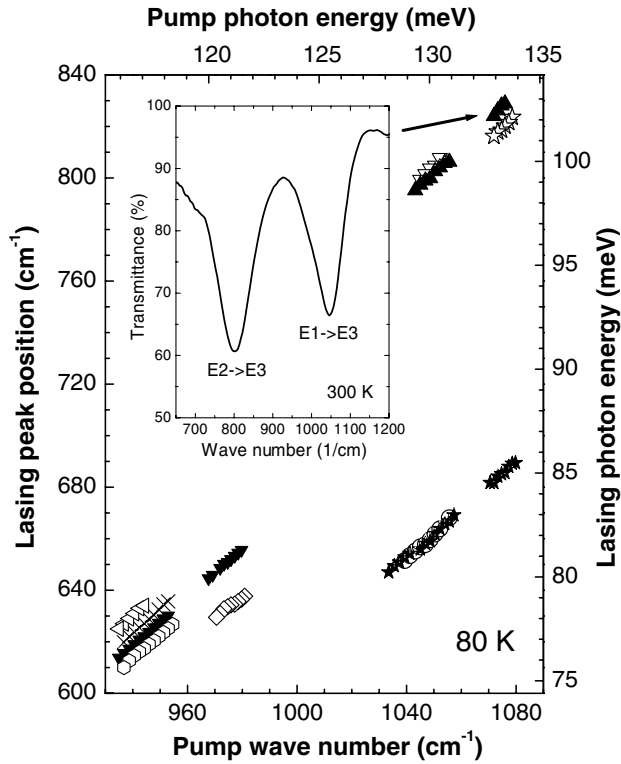


FIG. 2. Emission peak position versus pump position at 80 K. Each type of symbol represents one sample. The inset shows the transmission spectrum for one sample (indicated by the arrow) at room temperature under a multipass  $45^\circ$  geometry.

account the known temperature effect. In order to observe the 2-to-3 absorption, we must use a higher temperature than 80 K to populate the  $E_2$  subband.

The experimental results shown in Fig. 3 clearly indicate that there are two inaccessible regions in the neighborhood of the phonon energies, indicated by the two horizontal lines. Given the fact that the intersubband transition is a fully collective and resonant process and causes not only an absorption but also a change in the real part of the dielectric constant, we consider the following coupled-mode picture, analogous to the well-known electron plasmon-phonon problem [12]. It has been well established that coupled-mode formation in semiconductor materials can be treated in the linear-response approximation [12,15]. Hence, in the present case also we take the contributions of intersubband transitions and phonons to the dielectric additive. The coupled-mode solutions are found by setting the real part to zero:

$$\text{Re}[\epsilon_{\text{IT}}(\omega) + \epsilon_{\text{phonon}}(\omega)] = 0, \quad (1)$$

where the intersubband transition contribution is

$$\epsilon_{\text{IT}}(\omega) = \epsilon_0 \epsilon_\infty \frac{\omega_{\text{IT}}^2}{\omega_{12}^2 - \omega^2 - i\omega 0^+}, \quad (2)$$

the phonon contribution is

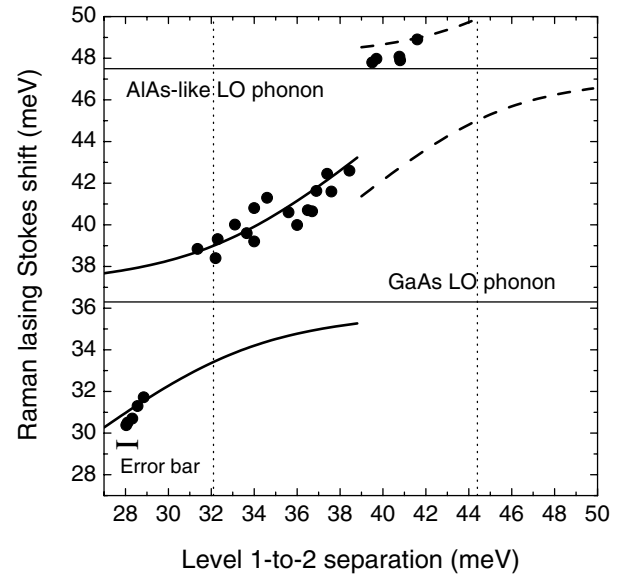


FIG. 3. Difference between pump and emission photon energies (i.e., the Stokes Raman shift) versus level 1 and level 2 separation. The curves (solid for GaAs phonon and dashed for AlAs-like mode of AlGaAs) are calculated from the coupled-mode model. The two horizontal lines indicate the positions of the LO phonons, while the two vertical dotted lines show the expected anticrossing positions, 32.1 and 44.4 meV shifted from the phonon energies (36.3 and 47.5 meV) by the depolarization effect. All experimental data points have an error bar of about 1 meV in the  $x$  axis, whereas the uncertainty in the  $y$  axis is negligible (less than 0.1 meV).

$$\epsilon_{\text{phonon}}(\omega) = \epsilon_0 \epsilon_\infty \frac{\omega_{\text{LO}}^2 - \omega^2}{\omega_{\text{TO}}^2 - \omega^2 - i\omega 0^+}, \quad (3)$$

$\omega_{\text{IT}} = e^2 n_{3\text{D}} f_{12} / \epsilon_0 \epsilon_\infty m^*$ ,  $m^*$  is the effective mass,  $\omega_{12}$  is the 1-to-2 level separation,  $\omega_{\text{TO/LO}}$  is the TO- or LO-phonon frequency,  $\epsilon_0$  is the vacuum permittivity,  $\epsilon_\infty$  is the high frequency dielectric constant, and  $0^+$  is the damping or width parameter which is set to zero.

There are small uncertainties in most of the parameters: The oscillator strength  $f_{12}$  (approximately unity for the 1-to-2 transition) can be easily calculated, and the phonon frequencies are well known. The three-dimensional carrier density  $n_{3\text{D}}$  is taken to be the modulation doping density spread over the DQW, i.e., about  $2 \times 10^{17} \text{ cm}^{-3}$ . The curves (solid for GaAs and dashed for AlAs-like phonon) in Fig. 3 are the results of solving Eq. (1) for the two phonons. The agreement with experiment is evident. Note also that each point in Fig. 3 represents one sample, and therefore a large number of samples have been characterized. Equation (1) can be easily solved analytically, resulting in two solutions for the coupled modes. Simple manipulations show that the anticrossing point is not at  $\omega_{12} = \omega_{\text{LO}}$  as would be anticipated but at  $\omega_{12}^2 = \omega_{\text{LO}}^2 - \omega_{\text{IT}}^2$ . For the GaAs phonon (36.3 meV), this point is calculated to be 32.1 meV, in acceptable agreement with experiment (see Fig. 3). The coupled-mode analysis

[Eqs. (1)–(3)] is an approximation that includes the leading term in the collective excitation. This is the dynamic Coulomb correction, i.e., related to the depolarization effect. It is interesting to note the quantity  $\omega_{IT}$  is equivalent to the depolarization shift commonly seen in the literature [20]. A similar linear-response model formulation is used in Ref. [15]. A rigorous approach would involve calculating the response function, similar to that described in Mahan [21]. From such a derivation, it is apparent that the expression given here is the (leading) linear term.

Obviously the simple model employed here is mainly to show the essential physics and for easy understanding and presentation. It is by no means a complete theory. The full solution to the problem would involve solving the full three-level problem in the presence of the phonon modes, the strong pumping field, and the lasing field. Moreover, the intersubband transition causes an anisotropy in the dielectric function. The effect is important in modeling the electromagnetics, for example, calculating the modes of the laser waveguides. The simple model does provide a qualitative and physical understanding. The new coupled-mode picture, in contrast with the conventional (pure phonon) Raman scattering process, is as follows. Although both are inelastic light scattering processes, the fundamental difference is that the conventional picture leaves the system in a state of one extra phonon, whereas the new picture ends with the generation of a coupled-mode excitation. We are not aware of other clear observations on resonantly coupled intersubband-phonon modes.

In conclusion, we have reported detailed experimental evidence of coupled modes of collective intersubband transitions and LO phonons in Raman lasing experiments in an artificial three-level system. Our initial picture from earlier experiments [9] of a pure phonon process is hereby modified, and a new picture of lasing mediated by a coupled intersubband-phonon mode is proposed. The strong coupling effect is important in the understanding and design of various intersubband infrared lasers, such as QCLs. This work could open up a new avenue for realizing a phonon or even a polaron “laser” that was proposed by Wolff [22] over 30 years ago and discussed again more recently [23].

We thank E. Dupont and P. Hawrylak for discussions and J. Fraser and S. Rolfe for SEM and SIMS measurements, respectively.

---

\*Electronic address: h.c.liu@nrc.ca

[1] J. Faist, F. Capasso, D.L. Sivco, C. Sirtori, A.L. Hutchinson, and A.Y. Cho, *Science* **264**, 553 (1994).

- [2] R. Paiella, F. Capasso, C. Gmachl, D.L. Sivco, J.N. Baillargeon, A.L. Hutchinson, A.Y. Cho, and H.C. Liu, *Science* **290**, 1739 (2000).
- [3] C. Gmachl, D.L. Sivco, R. Colombelli, F. Capasso, and A.Y. Cho, *Nature (London)* **415**, 883 (2002).
- [4] J. Faist, F. Capasso, C. Sirtori, D.L. Sivco, and A.Y. Cho, in *Intersubband Transition in Quantum Wells: Physics and Device Applications II*, Semiconductors and Semimetals Vol. 66, edited by H.C. Liu and F. Capasso (Academic, San Diego, 2000), Chap. 1, pp. 1–83.
- [5] F. Capasso, R. Paiella, R. Martini, R. Colombelli, C. Gmachl, T.L. Myers, M.S. Taubman, R.M. Williams, C.G. Bethea, K. Unterrainer, H.Y. Hwang, D.L. Sivco, A.Y. Cho, M.A. Sergent, H.C. Liu, and E.A. Whittaker, *IEEE J. Quantum Electron.* **38**, 511 (2002).
- [6] O. Gauthier-Lafaye, P. Boucaud, F.H. Julien, S. Sauvage, J.M. Lourtioz, V. Thierry-Mieg, and R. Planel, *Appl. Phys. Lett.* **71**, 3619 (1997).
- [7] O. Gauthier-Lafaye, F.H. Julien, S. Cabaret, J.M. Lourtioz, G. Strasser, E. Gornik, M. Helm, and P. Bois, *Appl. Phys. Lett.* **74**, 1537 (1999).
- [8] H.C. Liu and A.J. SpringThorpe, *Phys. Rev. B* **61**, 15 629 (2000).
- [9] H.C. Liu, I.V. Cheung, A.J. SpringThorpe, C. Dharma-wardana, Z.R. Wasilewski, D.J. Lockwood, and G.C. Aers, *Appl. Phys. Lett.* **78**, 3580 (2001).
- [10] C.K.N. Patel and E.D. Shaw, *Phys. Rev. Lett.* **24**, 451 (1970).
- [11] C.K.N. Patel, E.D. Shaw, and R.J. Kerl, *Phys. Rev. Lett.* **25**, 8 (1970).
- [12] A. Mooradian and A.L. McWhorter, *Phys. Rev. Lett.* **19**, 849 (1967).
- [13] I.W. Johnstone, D.J. Lockwood, G. Mischler, J.R. Fletcher, and C.A. Bates, *J. Phys. C* **11**, 4425 (1978).
- [14] G. Abstreiter and K. Ploog, *Phys. Rev. Lett.* **42**, 1308 (1979).
- [15] A. Pinczuk, J.M. Worlock, H.L. Stormer, R. Dingle, W. Wiegmann, and A.C. Gossard, *Solid State Commun.* **36**, 43 (1980).
- [16] B. Jusserand and J. Sapriel, *Phys. Rev. B* **24**, 7194 (1981).
- [17] Z.R. Wasilewski, M.M. Dion, D.J. Lockwood, P. Poole, R.W. Streater, and A.J. SpringThorpe, *J. Appl. Phys.* **81**, 1683 (1997).
- [18] S. Yu, K.W. Kim, M.A. Stroschio, G.J. Iafrate, J.-P. Sun, and G.I. Haddad, *J. Appl. Phys.* **82**, 3363 (1997).
- [19] H.B. Teng, J.P. Sun, G.I. Haddad, M.A. Stroschio, S. Yu, and K.W. Kim, *J. Appl. Phys.* **84**, 2155 (1998).
- [20] W.P. Chen, Y.J. Chen, and E. Burstein, *Surf. Sci.* **58**, 263 (1976).
- [21] G.D. Mahan, *Many-Particle Physics* (Kluwer, New York, 2000), pp. 467–475.
- [22] P.A. Wolff, *Phys. Rev. Lett.* **24**, 266 (1970).
- [23] F. Fuchs, H. Schneider, P. Koidl, K. Schwarz, H. Walcher, and R. Triboulet, *Phys. Rev. Lett.* **67**, 1310 (1991).